The SH3 domain acts as a scaffold for the N-terminal intrinsically disordered regions of c-Src

Mariano Maffei[1], Miguel Arbesú[1], Anabel-Lise Le Roux[1,2], Irene Amata[1,4], Serge Roche[3] and Miquel Pons[1*]

[1]BioNMR laboratory, Organic Chemistry Department, Universitat de Barcelona, Baldiri Reixac 10-12, 08028 Barcelona, Spain.

[2]Institute for Research in Biomedicine (IRB Barcelona). Baldiri Reixac, 10-12, 08028 Barcelona, Spain.

[3]CNRS UMR5237, University of Montpellier, CRBM, 1919 route de Mende, 34000 Montpellier, France.

[4]*Present address:* Institut de Biologie Physico-Chimique, 13 rue Pierre et Marie Curie, 75005 Paris, France.

* *Corresponding author:* mpons@ub.edu

SUMMARY

Regulation of c-Src activity by the intrinsically disordered Unique domain has been recently demonstrated. However, its connection with the classical regulatory mechanisms is still missing. Here we show that the Unique domain is part of a long loop closed by the interaction of the SH4 and SH3 domains. The conformational freedom of the Unique domain is further restricted through direct contacts with SH3 that are allosterically modulated by binding of a poly-proline ligand in the presence and in the absence of lipids. Our results highlight the scaffolding role of the SH3 domain for the c-Src N-terminal intrinsically disordered regions and suggest a

connection between the regulatory mechanisms involving the SH3 and Unique domains.

INTRODUCTION

The non-receptor protein kinase c-Src was the first discovered proto-oncogene and it plays a critical role in mediating signal transduction in multiple pathways (Martin, 2001) related with cell migration, invasion and survival, all of which contribute to its oncogenic potential. High levels of c-Src activity have been associated to poor prognosis in colorectal, prostate and breast cancers (Sirvent et al., 2012; Yeatman, 2004; Hynes, 2000). However, c-Src mutations are seldom found in cancer cells, suggesting that the transforming potential is associated to failures in c-Src regulation.

c-Src domain structure, which is shared with the other members of the Src family of kinases (SFKs), consists of four “Src-homology” domains: SH4, SH3, SH2 and SH1, arranged in this order from the N-terminus to the C-terminus, with the “Unique” domain separating the SH4 and SH3 domains (Figure 1A). The SH1 domain is the enzymatically active kinase domain. The SH4 domain contains lipid substitutions and is primarily responsible for anchoring the SFKs to membranes. In the case of c-Src it contains a myristoyl group attached to the N-terminus. Positively charged residues in the SH4 domain also contribute to the interaction with negatively charged membranes (Resh, 1999). The Unique domain is intrinsically disordered and also has the capacity to interact with lipids, other proteins, such as calmodulin, and the adjacent SH3 domain (Perez et al., 2013).

The SH3 and SH2 domains are regulatory domains. The interaction of the SH2 domain with a phosphorylated tyrosine located near the C-terminus contributes to maintain c-Src in a closed basal state that is enzymatically inactive. The viral forms of Src (v-Src) missing the C-terminal tyrosine are constitutively active (Martin, 2001) but various v-Src forms display different levels of activity indicating additional levels of regulation (Reddy et al., 1990; Brábek et al., 2002). Structurally, the Y530F mutant of human c-Src remains 85% in its closed form (Bernadó et al., 2009). This second layer of regulation has been associated to interactions involving the SH3 domain, including binding to a proline-rich region in the linker connecting the SH2 and SH1 domains (Xu et al., 1999), as well as interactions not related to poly-proline binding and involving the nSrc and RT-loops (Brábek et al., 2002).

SH3 domains are one of the most abundant domain families in eukaryotes, with about 300 occurrences in the human genome (Karkainen et al., 2006). SH3 domains are small (60-70 residues) and consist in a β-sandwich formed by five or six β-strands connected by three loops (the RT, nSrc and distal loops) and a short 3_{10} helix (Figures 1B, 1C).

In addition to the canonical interaction with PxxP sequences (Cheadle et al., 1994; Rickles et al. 1994; Feng et al., 1995), the SH3 domain of c-Src interacts with lipids and the Unique domain (Perez et al., 2013). The SH3 residues directly interacting with PxxP segments and the Unique domain are located in opposite sides of the domain. However, binding of a high affinity poly-proline peptide to the SH3 domain allosterically modulates the interaction with the Unique domain (Perez et al., 2013).

The functional role of the Unique domain has remained obscure until very recently. Residues 60-67 in the Unique domain form the Unique lipid binding region (ULBR) (Figure 1B) with residual structure even in the isolated domain (Perez et al., 2009).

Lipid binding was abolished by replacing residues 63-65 (LFG) by three alanines (Perez et al., 2013). This mutation, which we refer to as AAA, causes strong phenotypes when introduced in full-length c-Src and expressed in *Xenopus laevis* oocytes (Perez et al., 2013) or in human colorectal cancer cells (unpublished).

These results strongly suggest that the Unique domain forms a new layer of regulation for c-Src but raise the question of how this new regulation mechanism is connected with the classical ones, involving the SH3 and SH2 domain. Figure 1A summarizes the previously and newly described regulatory interactions and highlights the central role of the SH3 domain. In this work we show the SH3 domain acting as scaffold for the intrinsically disordered Unique domain, the interaction between the SH3 and the SH4 domains closing a long loop including the entire Unique domain, the direct interaction of the SH3 domain with lipids, and the allosteric modulation of SH3 binding to the Unique domain and lipids by its canonical interaction with a poly-proline peptide.

RESULTS

Interaction of SH3 with the Unique and SH4 domains of c-Src

NMR chemical shift perturbations (CSP) were used to map the residues affected by the interaction between SH3 and the disordered regions of c-Src (USrc = SH4 + Unique domains). They were determined by comparing ^{1}H-^{15}N HSQC NMR spectra of a linked multi-domain construct (USrc-SH3, residues 1-150) with those of shorter peptides, containing the individual components (USrc, residues 1-85; SH3, residues 86-150). The peptides and proteins used are summarized in Table 1. Figure 2 shows

the sequence-specific combined ^{15}N and ^{1}H CSP measured at pH 7.0. Figure 2A shows the results for the disordered regions measured at 278 K to minimize proton amide exchange. Disregarding amino acids close to the linkage region (83-89), T37, A55, E60, K62 and N68 in the Unique domain and K5, S6 in the SH4 domain are the most affected residues. Residues 2 to 4 are not observable due to fast exchange at this pH and temperature. Figures 2B show the SH3 residues whose chemical shifts are affected by the presence of the Unique and SH4 domains at 298 K. The main changes in the SH3 domain are observed in the nSrc loop, around V114, and the RT loop (R98, D102). Perturbations are also observed in residues around H125 and T132 flanking the distal loop, and in residues located in the 3_{10} helix and the C-terminal region.

SH3 domains recognize poly-proline sequences. The binding site is formed mainly by aromatic residues on the SH3 surface (highlighted in Figures 1B and 1C) but ligand binding effects propagate across the SH3 domain through a hydrogen bond network, (Wang et al., 2001; Cordier et al., 2000) extending to the RT-loop and residues located on the opposite side of the poly-proline ligand binding site. We had previously reported the allosteric modulation of Unique domain binding by the addition of a poly-proline peptide (PPP) with the sequence Ac-VSLARRPLPPLP-OH, which is a consensus high affinity SH3 ligand (Perez et al., 2013; Feng at al., 1995). Interestingly, the interaction between the SH3 domain and residues in the SH4 domain is not affected by the presence of the PPP ligand. This is clearly seen in Figure 2C in which similar large chemical shifts differences for residues K5 and S6 are observed between USrc and USrc-SH3 in the presence and in the absence of PPP. In contrast, many of the Unique domain residues that were most affected by the interaction with the SH3 domain (T37, A55, E60, K62) have very similar chemical

shift values in USrc and USrc-SH3 in the presence of the PPP ligand, indicating that those amino acids sense an environment similar to that of USrc.

Chemical shifts differences of SH3 residues in the SH3-PPP complex and in the USrc-SH3-PPP complex map the regions of the SH3 domain that are interacting with USrc in the presence of the PPP ligand. Figure 2D clearly shows that the interactions involving the nSrc loop are retained, while most of the other interacting regions disappear in the SH3-PPP complex. Since only the N-terminal region of the SH4 domain retains its interaction in the presence of PPP it can be concluded that this region of the SH4 domain interacts with the nSrc loop of SH3 in the SH3-PPP complex. The similar chemical shifts of residues K5 and S6 in the apo and PPP-bound forms of USrc-SH3 suggest that these residues are also interacting with the nSrc loop in the apo protein, and that the RT-loop interacts with the Unique domain in the absence of the PPP ligand but this interaction is lost in the PPP complex. The regions of the SH3 domain interacting with the disordered domains in the absence and in the presence of PPP are indicated in Figures 2E and 2F.

The USrc region is covalently connected to the SH3 domain but also anchored to the SH3 domain by the N-terminal part of the SH4 domain closing a 78-residues long loop including the remaining residues of the SH4 domain and the complete Unique domain. Additional contacts between residues in the Unique domain and SH3 further decrease its conformational freedom. The contacts with the Unique domain are lost in the PPP complex but a flexible loop is retained. The chemical shifts of NH groups of residues in the hinge region connecting the SH3 and Unique domains (residues S75-G85) are clearly affected by PPP binding to SH3 probably reflecting local changes caused by the loss of interactions along the Unique domain affecting the overall loop geometry.

The Unique domain directs the interaction site of SH4 in the SH3 domain

The interaction between the SH4 and SH3 domains was confirmed using a synthetic peptide with the sequence of the SH4 domain (SH4 peptide, residues 2-19, GSNKSKPKDASQRRRSLE).

Figure 3A shows the chemical shifts perturbations induced by the addition of a 10-fold excess of SH4 peptide to 100 μM SH3. In this experiment the most perturbed residues are located in the RT-loop, with the charged residues R98, E100 most affected. Additional effects are observed in residues located or flanking the distal loop (H125, G130, T132), with minor effects observed in the nSrc loop. The nSrc loop is the most perturbed region of the SH3 domain when the SH4 and SH3 domains are connected by the Unique domain, both in the presence and in the absence of PPP peptide. The addition of SH4 peptide to the complex formed between SH3 and PPP, induces chemical shift changes in the RT loop that are much smaller than in the case of apo-SH3 (Figure 3C). However, the effects in the nSrc and distal loop are similar and very small, in contrast to the large chemical shift changes in the nSrc loop observed when the PPP complexes of SH3 and USrc-SH3 are compared (Figure 2D). Thus, the Unique domain facilitates the interaction between the SH4 and nSrc loop both in the apo forms, where the Unique domain directly interacts with the SH3 domain, and in the PPP complex, where the direct Unique-SH3 interaction is lost.

The capacity of a 78-residue flexible peptide chain to determine the interaction site of the SH4 domain is a surprising result, considering the intrinsically disordered nature of the Unique domain. Previous NMR studies of the USrc protein had confirmed its

intrinsically disordered nature but had identified a short segment between residues 60 and 75 with residual structure (Perez et al., 2009). We decided to use a previously designed mutant, (Perez et al., 2013) in which residues 63-65 (LFG) had been replaced by alanines (AAA) to investigate the effects of Unique domain residual structure.

The AAA Unique domain mutant retains the interactions with the SH3 domain

Figure 4 shows plots of sequence dependent chemical shift differences obtained by comparing USrc-SH3-AAA, USrc-AAA and SH3 following the same approach used for the wild type construct (cf. Figure 2).

The perturbations induced by the WT and AAA forms of USrc in the NH chemical shifts of SH3 residues are similar. In particular, residues around V114, in the nSrc loop are the most perturbed also in the AAA mutant (cf. Figures 2B and 4B). The RT loop is also affected, although R98 and D102 show smaller chemical shift changes than in the wild-type construct. Small reductions on the chemical shift changes are also observed in the other loops although, overall, the same regions are affected.

USrc residues outside the mutation site show a very similar perturbation profile in the WT and AAA forms (cf. Figures 2A and 4A), confirming that the AAA mutation preserves most of the interaction sites between the Unique and SH3 domains, although the overall interaction is weaker.

Chemical shift differences may originate from direct contacts or indirect effects. To confirm the interaction between the Unique and SH3 domains we used Paramagnetic Relaxation Enhancement (PRE) by a paramagnetic centre (MTSL)

attached to a cysteine residue introduced at position 59 (close to the ULBR) of the WT and AAA mutants of USrc-SH3 constructs.

Proximity of the unpaired electron centre induces fast relaxation of the NMR signals, which translates into line broadening and decreased intensity. A reference spectrum is obtained by reducing the spin-label with an excess of ascorbic acid. Results are presented as the intensity ratio between the oxidized and reduced samples.

Figure 5 compares the PRE effects of a spin-label located at position 59 of the Unique domain in WT and AAA USrc-SH3. The most affected regions in the SH3 domain (highlighted) are similar. Residues in the distal loop and the RT-loop are less affected by the spin label in the AAA mutant than in the WT, in agreement with the chemical shift perturbation results.

Long-range intra-domain contacts in the Unique domain are perturbed in the AAA mutant

PRE effects on NH signals of peaks within the Unique domain show a complex pattern indicative of long-range contacts that is different for the WT and AAA proteins. In order to focus on the interactions within the USrc region, independently of additional interactions with the SH3 domain, we measured PREs in the isolated WT and AAA forms of USrc (Figures 6A, 6B). The PRE pattern as a function of the position along the sequence in the WT protein is not compatible with that expected for a random coil, indicated by the continuous grey line. Deviations from the predictions of the ideal-random coil model are lower in the AAA mutant than in WT USrc, suggesting that residues replaced by the AAA mutation have a direct influence

in the restricted conformational space (as compared to a random coil) sampled by the isolated Unique domain.

Lipid binding by USrc-SH3: de-convoluting lipid and inter-domain interactions using PPP binding

The SH3 domain binds to lipids through the RT- and nSrc loops. The affected residues are the same in the isolated SH3 domain (Perez et al., 2013), USrc-SH3 WT and USrc-SH3 AAA (Figure S1).

Since PPP binding to SH3 affects the RT-loop, we tested its effect on lipid binding. Figures 7A and 7B show the result of adding DHPC-DMPG bicelles in the NH chemical shifts of the apo- and PPP-bound forms of USrc-SH3. PPP binding nearly completely abolished direct lipid interaction of the SH3 domain but preserved those of residues 64-67 (ULBR) and 14-17 in the C-terminal part of the SH4 domain.

However, while the chemical shifts of NH groups from ULBR residues of USrc-SH3 in the presence of PPP but without lipids are the same as in USrc, the corresponding chemical shifts of the USrc-SH3-PPP complex in the presence of lipids do not coincide with those of USrc bound to lipids. These observations suggest that, although direct interaction of the ULBR with the SH3 domain is lost in the PPP complex, lipid binding by the ULBR is affected by the proximity of the SH3 domain.

This observation is consistent with the retention of the interaction of the SH4-SH3 interaction in the PPP complex.

Residues T37 and K62 interact with apo-SH3 but not with lipids. In the PPP complex these residues show the same chemical shift as in USrc confirming that PPP abolishes the direct interaction of the Unique and SH3 domains also in the presence

of lipids. The chemical shifts of residues A55 and E60 in the absence of PPP are affected by the addition of lipids (Figures 7B, S2) and also by the interaction with the SH3 domain (Figure 2A). In the PPP complex, both interactions are abolished. Thus PPP binding prevents the lipid interaction of residues 55 and 60 but not that of the ULBR. Residues 72 and 78 are perturbed by the addition of lipids only in the PPP complex. Considering that these residues are close to the Unique domain-SH3 hinge region, it is unclear whether the observed chemical shift changes represent direct lipid interactions or variations in the conformation of the hinge region induced by the interaction of the SH4 and ULBR with the lipid surface.

Figures 7C and 7D show the effect of adding PPP to USrc-SH3 in the presence of bicelles. Residues in the hinge region (72-85) are also strongly perturbed by PPP binding (Figure 7C). Those residues experience chemical shift perturbations of the same order as those observed by USrc-SH3-PPP binding in the absence of lipids (Figure 2C) suggesting that the 78-residue loop formed by the interaction between the SH4 and SH3 domains is preserved in the presence of lipids and its conformational space is affected when the additional contacts with the Unique domain are eliminated in the PPP complex.

Chemical shifts of the SH4 and SH3 residues that are mutually interacting in the absence of lipids are a good monitor for the persistence of this interaction. For example, the absence of chemical shift changes upon addition of PPP indicates that the SH3-SH4 interaction in conserved. The addition of PPP has the further effect to eliminate direct interactions between the SH3 and lipids. Therefore, the absence of chemical shifts in the SH3 region of USrc-SH3-PPP complex in the presence of lipids (Figure 7B) is an additional indication of the conservation of the Unique domain loop. Similarly, the chemical shifts of residues 6 and 7 of the SH4 domain in the presence

of lipids and PPP are very similar to those observed in the absence of lipids confirming that the SH4-SH3 interaction is preserved in the presence of lipids.

The SH4 domain is known to be the primary anchoring site of c-Src to membranes but we have shown that also interacts with the SH3 domain. This raises the question of how SH4 binding to lipids and the SH3 domain affect each other.

The SH4 domain includes the first 19 residues of c-Src. However, from our data, it appears to be composed of two regions (nSH4 and cSH4). Residues 5-7 (and possibly the preceding, not observed residues) form the N-SH4 sub-domain that binds the SH3 domain and are only marginally affected by lipids (at least in the not-myristoylated constructs). Residues 12-17 constitute the cSH4 sub-domain that shows the largest perturbations in the presence of negatively charged lipids (Figure 7A). In the USrc-SH3-PPP complex the interaction of cSH4 residues with lipids is maintained (and extended to include A21 in the Unique domain, Figure 7B). The chemical shifts of nSH4 residues are less affected by lipids and show similar changes in the apo and PPP-bound forms. The observed lipid-induced shifts in nSH4 may indicate that either this region is simultaneously interacting with lipids and the SH3 domain, or that they are affected by changes in the lipid-binding mode of the neighbour cSH4 sub-domain. In any case, the SH4 domain as a whole simultaneously interacts with lipids and the SH3 domain.

Interestingly, the boundary between nSH4 and cSH4 includes D10, the only negatively charged residue in the strongly positive charged domain. This residue together with its first neighbour A11, are not observable in the NMR spectra of USrc-SH3-PPP complex in presence of bicelles, probably due to exchange broadening as is often observed in hinge regions.

DISCUSSION

c-Src regulation through inter-domain interactions involving the folded SH2, SH3 and kinase domain, as well as the regulatory C-terminal tail has been extensively studied. The SH4 domain is mainly associated to the capacity of c-Src to interact with lipids, while the role of the intrinsically disordered Unique domain remains poorly understood, in spite of recent findings (Perez et al., 2013).

Here we have shown that the RT, nSrc and distal loops in the SH3 domain play a key role in the conformational properties of the flexible SH4 and Unique domain. We have also shown that binding of a poly-proline ligand to the SH3 domain allosterically affects the interactions involving the RT and nSrc SH3 loops, and therefore, directly influences the confomational space sampled by the Unique domain. Figure 8 shows a cartoon representation summarizing the contacts between the SH4, Unique and SH3 domains in absence and presence of lipids as well as the effect of PPP binding to the SH3 domain or the AAA mutation in the Unique domain.

The regulatory role of the Unique domain has been demonstrated by the phenotipic effects caused by the introduction of the AAA mutation in the full length protein expressed in a constitutively active form in *Xenopus laevis* oocytes and in colorectal SW620 cancer cells (unpublished). Regulatory inputs may include the known interactions of the Unique domain with lipids, with calmodulin (Perez et al., 2013), or its phosphorylation at various serine and threonine sites (Perez et al., 2009; Amata et al., 2013). How these imputs are converted in changes in the kinase activity or selectivity remains to be understood. The SH3 domain seems to be playing the role of an interaction hub connecting the flexible SH4 and Unique regions with the folded domain (SH1, SH2, SH3) cluster.

Independent evidence supporting the connection between the SH3 and Unique domains can be found by comparing the sequences of various v-Src forms (Table S1) in which, in addition to the missing regulatory tail, simultaneous mutations in the ULBR and the RT-loop of the SH3 domain are observed. These data are in agreement with the present NMR study indicating that the Unique domain preferentially interacts with the RT-loop.

The flexible SH4 and Unique domains of c-Src sample a restricted conformational space determined by long-range interactions including the SH3 domain. Ligand binding to the SH3 domain allosterically modulates some of these interactions but intra-domain contacts within the Unique domain are also important. The AAA mutation, which was experimentally observed to cause strong phenotypes when introduced in full-length c-Src, reduces some of these interactions leading to a more random-coil type conformation in the Unique domain. The same mutation destroys the Unique domain lipid binding region (Perez et al., 2013) but does not substantially modify the interactions of the Unique and SH4 domains with SH3 even in presence of a poly-proline peptide (Figure S3). Therefore, perturbation of the lipid binding remains the most probable mechanisms for the phenotypic effects of the AAA full-length mutant, although more subtle effects, related to its perturbation of the Unique domain conformational space cannot be ruled out.

Binding of a poly-proline ligand to the SH3 domain induces an allosteric regulation of the interactions involving the RT loop. Two of these interactions have been observed: binding of lipids by the SH3 domain and the interaction with the Unique domain. Interestingly, the interaction between the SH4 and SH3 domains in the USrc-SH3 construct is not affected by ligand binding and, therefore, the Unique domain is not completely released, although the direct contacts with the SH3 domain

are lost. This mechanism is conserved even when the molecule is interacting with lipid membranes. Thus, the SH3 domain remains close to the Unique domain and to the lipid surface even though the direct interactions with lipids or the Unique domain are lost. In the inactive form of c-Src the SH3 domain interacts with the proline rich segment connecting the SH2 and SH1 domains. This interaction is at least partially released when c-Src is activated. With the observed allosteric effects of PPP binding, is tempting to speculate on the possible “reverse” signalling in which the activation state of c-Src is transmitted to the flexible Unique and SH4 domains modulating their interaction with lipids.

EXPERIMENTAL PROCEDURES

Cloning and mutagenesis

The cDNA encoding for human c-Src SH4 and Unique domains (USrc, residues 1-85) plus a C-terminal Strep-tag® (*SAWSHPQFEK*) inserted for purification purposes, was cloned into a pET-14b vector (Novagene, UK). The human c-Src SH3 domain construct (SH3, residues 86-150) or bound to the c-Src N-terminal region (USrc-SH3, 1-150) was cloned into a pETM-30 vector (EMBL) after a TEV cleavage site and expressed as His_6-GST fusion proteins. Site-directed mutations were introduced using the QuikChange™ mutagenesis kit (Stratagene).

Protein expression and purification

The plasmids carrying the proteins of interest were transformed in Escherichia coli Rosetta^{TM}(DE3)pLysS cells (Novagen, UK). Cells were grown in M9 minimal medium supplemented with ^{15}N ($^{15}NH_4Cl$ from Cambridge Isotope Laboratories, UK). Protein

expression was carried out at 25ºC overnight after induction with 1 mM IPTG. Cells were then harvested and sonicated. USrc protein was purified from the cell lysate using Strep-tactin sepharose resin (IBA, Germany) and eluted with 2.5 mM of desthiobiotin. His_6-GST-SH3 and His_6-GST-USrc-SH3 constructs were recovered from cell lysate with Ni-NTA resin (Qiagen, Netherlands) and eluted with 400 mM imidazole. An overnight digestion with His-tagged TEV protease was performed at 4°C in order to remove the GST tag-protein. Imidazole was then removed from solution using PD-10 desalting columns (GE Healthcare, Spain). Digested products were incubated again with Ni-NTA resin at RT for 1hr. The flow-through containing only the protein of interest was collected.

Further purification was performed with size exclusion chromatography in a Superdex 75 26/60 column (GE Healthcare). For USrc constructs, 50 mM sodium phosphate buffer, 0.2 mM EDTA and 0.01% NaN_3 at pH 7.0 was used. For SH3 and USrc-SH3, the buffer was 50 mM sodium phosphate, 150 mM NaCl, 0.2 mM EDTA and 0.01% NaN_3 at pH 7.5. The protein-containing fractions were pooled, concentrated to the desired concentration (Centricon 5 kDa, Millipore, USA) and stored at 4ºC.

Further details about USrc purification protocols are described in Perez et al. (Perez et al., 2013[2]). Synthetic peptides SH4 and PPP were added as 40mM stock solutions in MilliQ H_2O to minimize dilution effects upon addition to the NMR samples.

NMR spectroscopy

After purification, all ^{15}N labelled samples were dissolved in 50 mM sodium phosphate buffer at pH 7.0 with 90% H_2O / 10% D_2O. Protein concentrations were in the range of 0.2 - 0.3 mM in all measurements.

All experiments were performed in a Bruker 600 MHz Advance III spectrometer equipped with a TCI cryoprobe (Unitat de RMN, Universitat de Barcelona, Spain). Either ^{1}H-^{15}N HSQC or ^{1}H-^{15}N SOFAST-HMQC (Schanda at al., 2005) experiments were carried out at pH 7.0 at 278 K, optimum for observing Unique domain signals, or 298 K, better suited to observe the SH3 domain and samples with lipid bicelles. NMR spectra were processed using Bruker TopSpin™ 3.0 and NMRPipe (Delaglio et al., 1995), and analysed using Sparky (Goddard and Kneller).

Combined chemical shift differences were calculated following the equation:

$$\Delta\delta = [(\Delta\delta H)^2 + (\Delta\delta N/5)^2]^{1/2} \qquad \text{Equation 1}$$

Individual chemical shifts differences larger than one standard deviation from the mean of all measured differences in the relevant pair of spectra were considered statistically significant.

USrc and USH3 assignments had been previously reported (Perez et. al., 2009; Perez et al., 2013). SH3 backbone assignment in presence of a poly-proline peptide was based on literature values (BRMB 4889) measured at pH 6.5 and 298 K.

Molecular images were generated using VMD 1.9.2 (Humphrey et al., 1996) or Chimera (Pettersen et al., 2004).

PRE experiments

The paramagnetic tag used for spin labelling was MTSL ((1-oxy-2,2,5,5-tetramethyl-D-pyrroline-3-methyl)-methanethiosulfonate). The cysteine-containing mutants were purified following the same previously described protocol with 5 mM DTT on each step to avoid disulphide-bond formation. For protein-tagging reaction, DTT was removed using a desalting PD-10 column and a 16-fold excess of MTSL was added

to the protein solution. After overnight reaction at 4ºC, the MTSL excess was eliminated using a desalting column.

Addition of a 5-fold excess of ascorbic acid to the protein solution was used to reduce the nitroxide radical and provided the control diamagnetic sample.

Theoretical PRE profiles were calculated using Flexible Meccano 1.1 (Ozenne et al., 2012). 50,000 conformer ensembles were generated for each construct. The intrinsic ^{1}H linewidth parameter was obtained from the average linewidth of the ^{1}H signals in the diamagnetic sample.

Lipid bicelle preparation

Negatively charged bicelles were prepared using a mixture of short chain (DHPC, dihexanoyl phosphatidylcholine) and long chain (DMPG, dimyristoyl phosphatidyl glycerol) lipids in a molar ratio of 1.0 DHPC : 0.8 DMPG (q = 0.8, 44.4% DMPG molar ratio), which provides isotopic fast tumbling bicelles (Glover et al., 2001; Vold et al., 1997). The lipids were dissolved in chloroform mixtures and the solvent was evaporated in vacuo. The resulting lipid film was rehydrated in 50 mM phosphate buffer at pH 7.0. The mixture was then vortexed and subjected to freeze and thaw cycles with vortexing and pipetting. Concentrated protein stocks and D_2O were then added to the clear bicelle solution to a final concentration of 8%(w/v) lipids, 0.2 mM protein and 10% D_2O.

Further details about bicelle preparation protocols are described in Perez et al. (Perez et al., 2013[2]).

Reagents and chemicals

Synthetic peptides SH4 (residues 2-19, GSNKSKPKDASQRRRSLE) and PPP (Ac-VSLARRPLPPLP-OH) were synthesized and purified by GenScript, USA.

IPTG was purchased to Melford, UK; MTSL paramagnetic tag was purchased to Toronto Research Chemicals, Canada; DHPC and DMPG lipids were purchased to Avanti Polar Lipids, USA; the rest of salts and reagents were purchased to Sigma.

AUTHOR CONTRIBUTIONS

M.P. conceived the overall project; M.M. and M.P. designed the experiments. M.M., M.A., I.A., A.L.L.R. produced the samples and performed the experiments. M.M., S.R. and M.P. wrote and revised the manuscript.

ACKNOWLEDGMENTS

This work was supported by funds from the Fundació Marató TV3 and the Spanish "Ministerio de Economia y Competitividad" (BIO2013-45993R, co-financed with structural funds (FEDER) from the European Union, and predoctoral fellowship to M.M.). A.L.L.R. holds a predoctoral fellowship from "La Caixa". I.A. was the recipient of a Marie Curie fellowship. S.R. is an INSERM investigator. We acknowledge the use of the LRB NMR facilities and the CCiT of the University of Barcelona. Chimera is developed by the Resource for Biocomputing, Visualization, and Informatics at the University of California, San Francisco (supported by NIGMS 9P41GM103311). The authors declare no competing financial interests.

REFERENCES

Amata, I., Maffei, M., Igea, A., Gay, M., Vilaseca, M., Nebreda, A.R., and Pons, M. (2013). Multi-phosphorylation of the intrinsically disordered unique domain of c-Src studied by in-cell and real-time NMR spectroscopy. Chembiochem *14*, 1820–1827.

Bernadó, P., Pérez, Y., Svergun, D.I., and Pons, M. (2008). Structural characterization of the active and inactive states of Src kinase in solution by small-angle X-ray scattering. J. Mol. Biol. *376*, 492-505.

Brábek, J., Mojzita, D., Novotny, M., Frantisek, P., and Folk, P. (2002). The SH3 domain of Src can downregulate its kinase activity in the absence of the SH2 domain-pY527 interaction. Biochem. Biophys. Res. Commun. *296*, 664–670.

Cheadle, C., Ivashchenko, Y., South, V., Searfoss, G.H., French, S., Howk, R., Ricca, G.A., and Jaye, M. (1994). Identification of a Src SH3 Domain Binding Motif by Screening a Random Phage Display Library. J. Biol. Chem. *269*, 24034–24039.

Cordier, F., Wang, C., Grzesiek, S., and Nicholson, L.K. (2000). Ligand-induced strain in hydrogen bonds of the c-Src SH3 domain detected by NMR. J. Mol. Biol. *304*, 497–505.

Delaglio, F., Grzesiek, S., Vuister, G.W., Zhu, G., Pfeifer, J., and Bax, A. (1995). J. Biomol. NMR *6*, 277–293.

Feng, S., Kasahara, C., Rickles, R.J., and Schreiber, S.L. (1995). Specific interactions outside the proline-rich core of two classes of Src homology 3 ligands. Proc. Natl. Acad. Sci. U. S. A. *92*, 12408–12415.

Glover, K.J., Whiles, J. a, Wu, G., Yu, N., Deems, R., Struppe, J.O., Stark, R.E., Komives, E. a, and Vold, R.R. (2001). Structural evaluation of phospholipid bicelles for solution-state studies of membrane-associated biomolecules. Biophys. J. *81*, 2163–2171.

Goddard, T.D., Kneller, D. G. SPARKY 3, University of California, San Francisco.

Humphrey, W., Dalke, A., and Schulten, K. (1996). VMD : Visual Molecular Dynamics. J Mol Graph *7855*, 33–38.

Hynes, N. E. (2000). Tyrosine kinase signalling in breast cancer. Breast Cancer Res. *2*, 154-157.

Kärkkäinen, S., Hiipakka, M., Wang, J.-H., Kleino, I., Vähä-Jaakkola, M., Renkema, G.H., Liss, M., Wagner, R., and Saksela, K. (2006). Identification of preferred protein interactions by phage-display of the human Src homology-3 proteome. EMBO Rep. *7*, 186–191

Martin, G.S. (2001). The hunting of the Src. Nat. Rev. Mol. Cell Biol. *2*, 467–475.

Ozenne, V., Bauer, F., Salmon, L., Huang, J.-R., Jensen, M.R., Segard, S., Bernadó, P., Charavay, C., and Blackledge, M. (2012). Flexible-meccano: a tool for the generation of explicit ensemble descriptions of intrinsically disordered proteins and their associated experimental observables. Bioinformatics *28*, 1463–1470.

Pérez, Y., Gairí, M., Pons, M., and Bernadó, P. (2009). Structural characterization of the natively unfolded N-terminal domain of human c-Src kinase: insights into the role of phosphorylation of the unique domain. J. Mol. Biol. *391*, 136–148.

Pérez, Y., Maffei, M., Igea, A., Amata, I., Gairí, M., Nebreda, A.R., Bernadó, P., and Pons, M. (2013). Lipid binding by the Unique and SH3 domains of c-Src suggests a new regulatory mechanism. Sci. Rep. *3*, 1295.

[2]Perez, Y., Maffei, M., Amata, I., Arbesú, M., and Pons, M. (2013). Lipid Binding by Disordered Proteins. Protocol Exchange DOI:10.1038/protex.2013.094

Pettersen, E.F., Goddard, T.D., Huang, C.C., Couch, G.S., Greenblatt, D.M., Meng, E.C., and Ferrin, T.E. (2004). UCSF Chimera - A visualization system for exploratory research and analysis. J. Comput. Chem. *25*, 1605–1612.

Reddy, S., Mazzu, D., Mahan, D., Shalloway, D. (1990). Sequence and Functional Differences between Schmidt-Ruppin D and Schmidt-Ruppin A Strains of pp60 v-src J. Virology. *64*, 3545-3550.

Resh, M.D. (1999). Fatty acylation of proteins: new insights into membrane targeting of myristoylated and palmitoylated proteins. Biochim. Biophys. Acta *1451*, 1-16.

Rickles, R.J., Botfield, M.C., Weng, Z., Taylor, J.A., Green, O.M., Brugge, J.S., and Zoller, M.J. (1994). Identification of Src, Fyn, Lyn, P13K and Abl SH3 domain ligands using phage display libraries. EMBO J. *13*, 5598–5604.

Schanda, P., Kupce, E., and Brutscher, B. (2005). SOFAST-HMQC experiments for recording two-dimensional heteronuclear correlation spectra of proteins within a few seconds. J. Biomol. NMR *33*, 199–211.

Sirvent, A., Benistant, C., and Roche, S. (2012). Oncogenic signaling by tyrosine kinases of the SRC family in advanced colorectal cancer. Am J Cancer Res *2*, 357–371.

Vold, R. R., Prosser, R. S. and Deese, A. J. (1997). Isotropic solutions of phospholipid bicelles: a new membrane mimetic for high-resolution NMR studies of polypeptides. J. Biomol. NMR *3*, 329–35.

Wang, C., Pawley, N.H., and Nicholson, L.K. (2001). The role of backbone motions in ligand binding to the c-Src SH3 domain. J. Mol. Biol. *313*, 873–887.

Xu, W., Doshi, a, Lei, M., Eck, M.J., and Harrison, S.C. (1999). Crystal structures of c-Src reveal features of its autoinhibitory mechanism. Mol. Cell *3*, 629–638.

Yeatman, T.J. (2004). A renaissance for SRC. Nat. Rev. Cancer *4*, 470–480.

FIGURE LEGENDS

Figure 1. Domain structure and amino acid sequence of USrc-SH3 of human c-Src. (A) Domain structure of c-Src and regulatory interactions. Classical interactions of the SH2 domain with phosphotyrosine, the SH3 domain with a proline rich connector linking SH2 and SH1, and of SH4 with lipids are indicated in black. New interactions reported here are shown in red. (B) Residues 1-85 (SH4 and Unique domains) are shown in black. Residues 86-150 (SH3 domain) are shown in grey. The secondary structure according to Wang et al., 2001 is represented on top of the sequence. c-Src SH3 residues that are in direct contact with the core sequences of poly-proline ligand (Feng et al., 1995) are highlighted in brown. SH4-domain = red; Unique Lipid Binding Region (ULBR) = light-blue; RT-loop = green; nSrc-loop = dark blue; distal-loop = gold. The SH4 domain is divided in two sub-domains (see text for details). (C) Crystal structure of the SH3 domain of human c-Src (Protein Data Bank ID code 4HXJ). The color code is the same as in part B.

Figure 2. SH3 inter-domain interactions. (A-D) Combined absolute value ^{1}H-^{15}N NMR chemical shift changes between linked and isolated domains. (A and C) USrc-SH3 versus USrc at 278 K. (B and D) USrc-SH3 versus SH3 at 298 K. C and D were measured in the presence of 1 equivalent of PPP while no SH3-ligand was added in A and B. K5* Δδ value is 0.18 ppm (A and C) and V86* Δδ value is 0.14 ppm (B) and 0.13 ppm (D). V114* Δδ value is 0.12 ppm. All spectra were measured at pH 7.0 and at a protein concentration of 0.2 mM. Combined NH chemical shift differences (Δδ)

were computed as in equation 1 (see Experimental Procedures). Grey circles indicate proline residues. The dashed line represents one standard deviation. SH3 residues perturbed by the presence of USrc in the absence (E) and in the presence of PPP (F) are highlighted on the SH3 structure (PDB entry 4HXJ).

Figure 3. SH3-SH4 domains interaction. (A) Combined absolute value ^{1}H-^{15}N NMR chemical shift changes between SH3 domain alone and in presence of a 10-fold excess of SH4 peptide. (B) SH3 residues perturbed by the presence of a 10-fold excess of SH4 peptide are highlighted on the SH3 structure (PDB entry 4HXJ). (C) ^{1}H-^{15}N NMR chemical shift perturbations between SH3-PPP complex and SH3-PPP in presence of a 10-fold excess of SH4 peptide. Combined NH chemical shift differences (Δδ) were computed as in equation 1 (see Experimental Procedures). Grey circles indicate proline residues. The dashed line represents one standard deviation.

Figure 4. ULBR mutations partially affect inter-domain interactions. Combined absolute value ^{1}H-^{15}N NMR chemical shift changes between linked and isolated domains measured at pH 7.0 (A) USrc-SH3-AAA versus USrc-AAA at 278 K, K5* Δδ value is 0.11 ppm (B) USrc-SH3-AAA versus SH3 at 298 K. V86* Δδ value is 0.14 ppm. Proline residues are shown as grey circles. Dashed lines correspond to one standard deviation.

Figure 5. PRE experiments in spin-labeled USrc-SH3 constructs. Intensity ratios of NH cross-peaks from MTSL-labeled A59C-USrc-SH3 WT (A) and A59C-USrc-SH3-AAA mutant (B), between paramagnetic (oxidized) and diamagnetic (reduced)

forms. The most affected regions in the SH3 domain are highlighted. M = MTSL; grey circles indicate proline residues.

Figure 6. Effect of AAA mutation on long range interactions within the Unique domain. Intensity ratios of NH cross-peaks from MTSL-labeled A59C-USrc WT (A), A59C-USrc-AAA mutant (B) between paramagnetic (oxidized) and diamagnetic (reduced) forms. The grey line corresponds to the theoretical PREs computed from the random-coil definition (see Experimental Procedures). M = MTSL; grey circles indicate prolines.

Figure 7. Effect of the Poly-Proline peptide on the SH3-lipid interaction. (A) Combined ^{1}H-^{15}N chemical shift changes of USrc-SH3 induced by the presence of 8% w/v of DHPC/DMPG bicelles. (B) Combined ^{1}H-^{15}N chemical shift changes between USrc-SH3 WT construct in presence of PPP and in presence of PPP + DHPC/DMPG bicelles. (C) Combined ^{1}H-^{15}N chemical shift perturbations between USrc-SH3 WT construct in presence of DHPC/DMPG bicelles and in presence of DHPC/DMPG bicelles + PPP (only USrc residues are shown). (D) Combined ^{1}H-^{15}N chemical shift changes between USrc-SH3 WT construct in presence of DHPC/DMPG bicelles and in presence of DHPC/DMPG bicelles + PPP (only SH3 residues are shown). Notice the expanded Δδ scale associated to PPP binding. Arrows mark SH3 residues known to be directly interacting with PPP (long for the core, short for additional regions). Grey circles indicate proline residues. The dashed line represents one standard deviation. See also Figure S2.

Figure 8. Cartoon models showing SH4-Unique-SH3 interactions. The grey sphere represents the SH3 domain. The black line corresponds to the Unique domain, which is connected to the back of the SH3 domain. Residues or regions experimentally detected to be involved in interactions are indicated. The yellow oval represents the lipid bicelle (not to scale). (A) USrc-SH3 WT. Residues E60 and N68 are located at the beginning and at the end of the ULBR respectively. (B) USrc-SH3 AAA. Most of the inter-domain contacts outside the ULBR are retained. This mutation also affects the conformational space sampled by USrc. (C) USrc-SH3-PPP complex. SH3-Unique contacts are abolished while N-SH4-SH3 interaction is maintained. (D) USrc-SH3 in presence of lipids. SH4, ULBR (USrc) and the RT and nSrc loops of SH3 are involved in lipid binding. USrc-SH3 contacts are conserved. (E) USrc-SH3-PPP complex in presence of lipids. Direct SH3-lipids interaction is abolished. ULBR and SH4 interact with lipids. The SH4-SH3 interaction is retained.

Table 1. Truncated forms of c-Src used in this study.

Acronym	Residues	Description	Modifications
USrc-SH3 WT	1-150	SH4-Unique-SH3	GA[a] at N-terminus
USrc-SH3-AAA	1-150	SH4-Unique-SH3	GA at N-terminus ^{63}LFG^{65} - ^{63}AAA^{65}
USrc-SH3-WT-MTSL	1-150	SH4-Unique-SH3	GA at N-terminus A59C - MTSL
USrc-SH3-AAA-MTSL	1-150	SH4-Unique-SH3	GA at N-terminus ^{63}LFG^{65} - ^{63}AAA^{65} A59C - MTSL
USrc WT	1-85	SH4-Unique	ST[b] at C-terminus

USrc-AAA	1-85	SH4-Unique	ST at C-terminus ^{63}LFG^{65} - ^{63}AAA^{65}
USrc-WT-MTSL	1-85	SH4-Unique	ST at C-terminus A59C - MTSL
USrc-AAA-MTSL	1-85	SH4-Unique	ST at C-terminus ^{63}LFG^{65} - ^{63}AAA^{65} A59C - MTSL
SH3	86-150	SH3	GA at N-terminus
SH4 peptide	2-19	SH4	-

[a] Residues located before Methionine 1 after TEV cleavage.

[b] ST= Strep-tag (SAWSHPQFEK).

Figure
Click here to download high resolution image

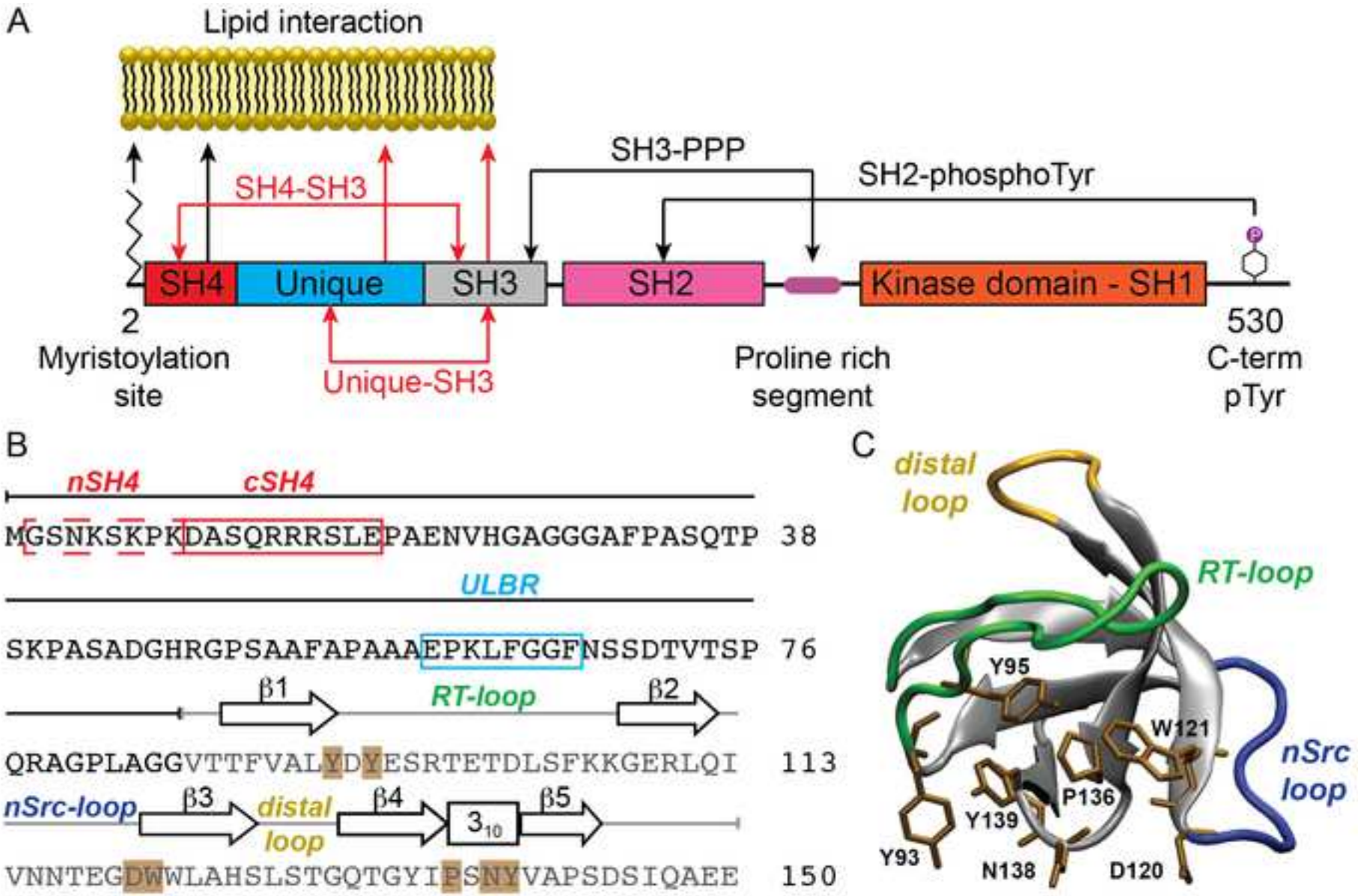

Figure
Click here to download high resolution image

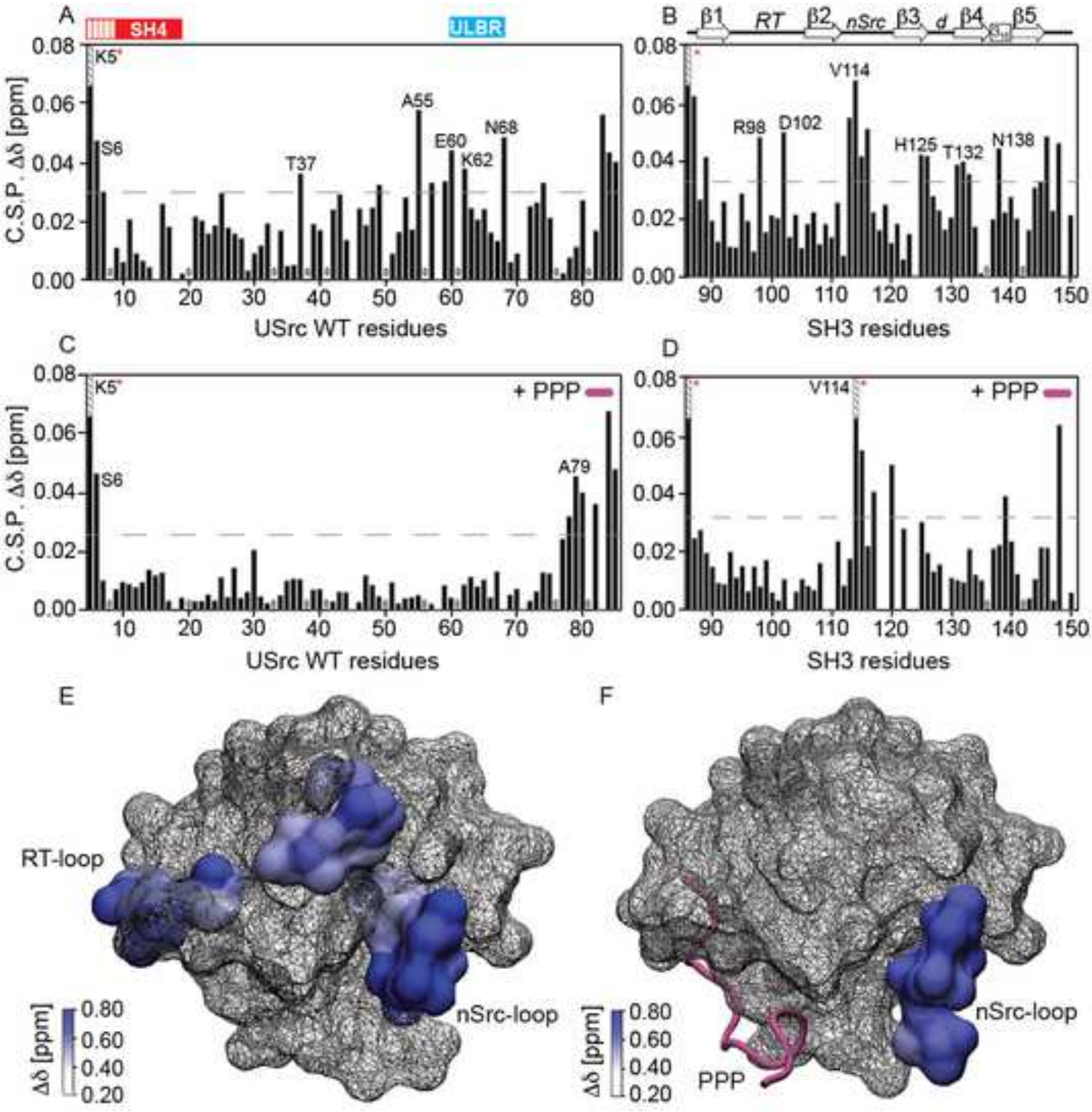

Figure
Click here to download high resolution image

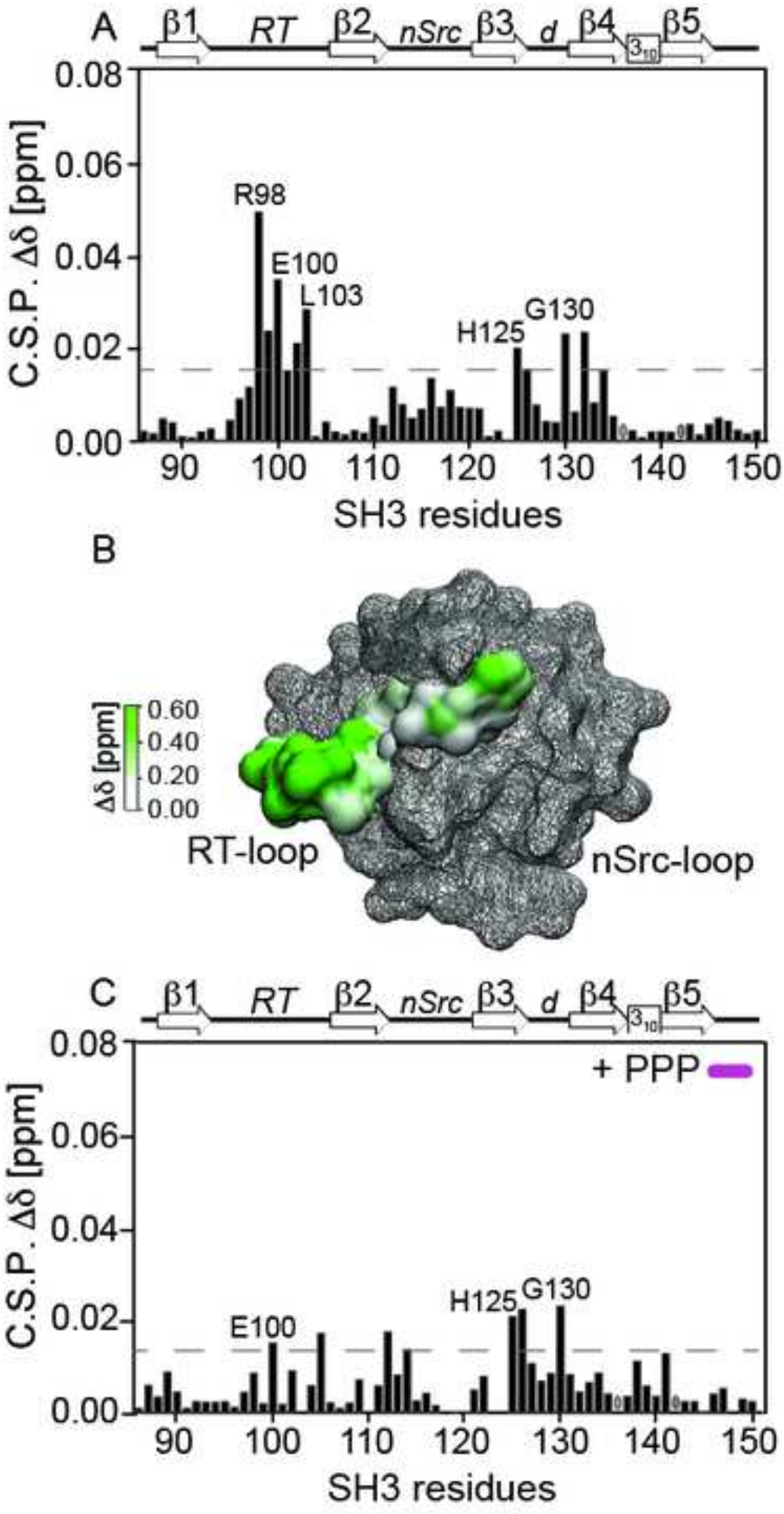

Figure
Click here to download high resolution image

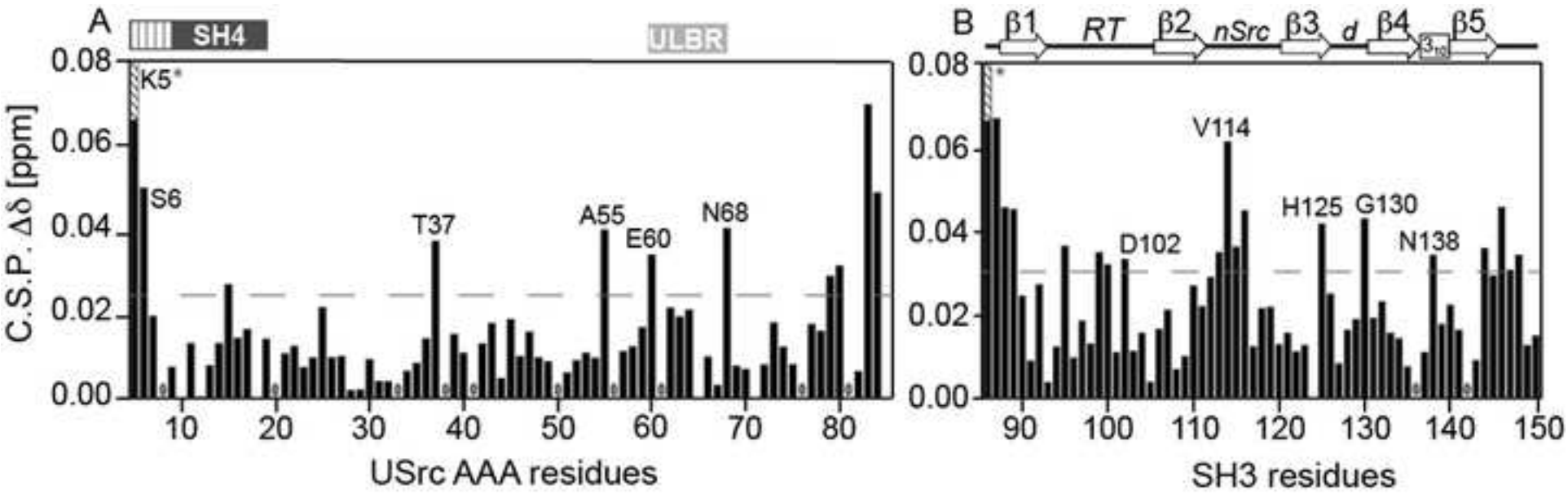

Figure
Click here to download high resolution image

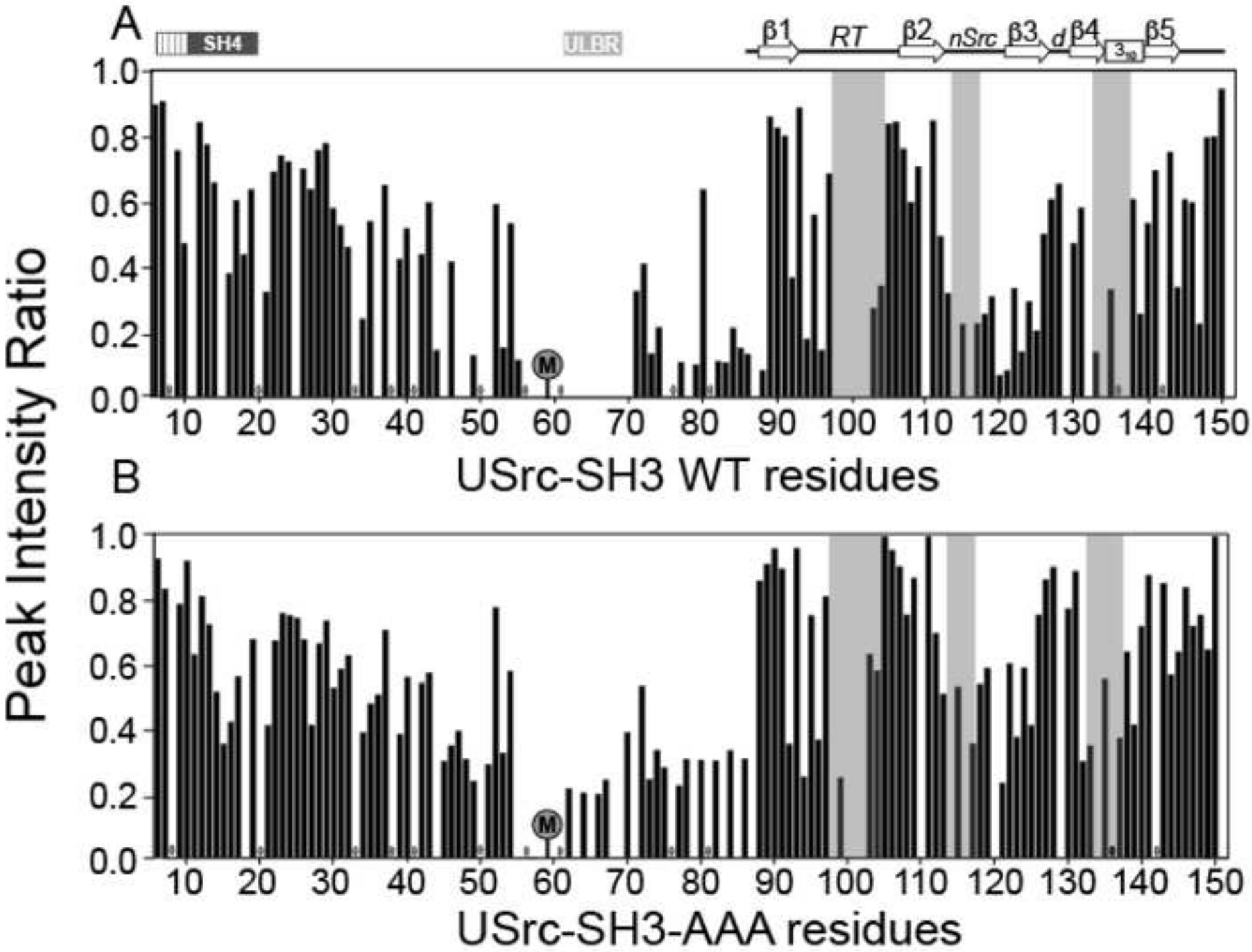

Figure
Click here to download high resolution image

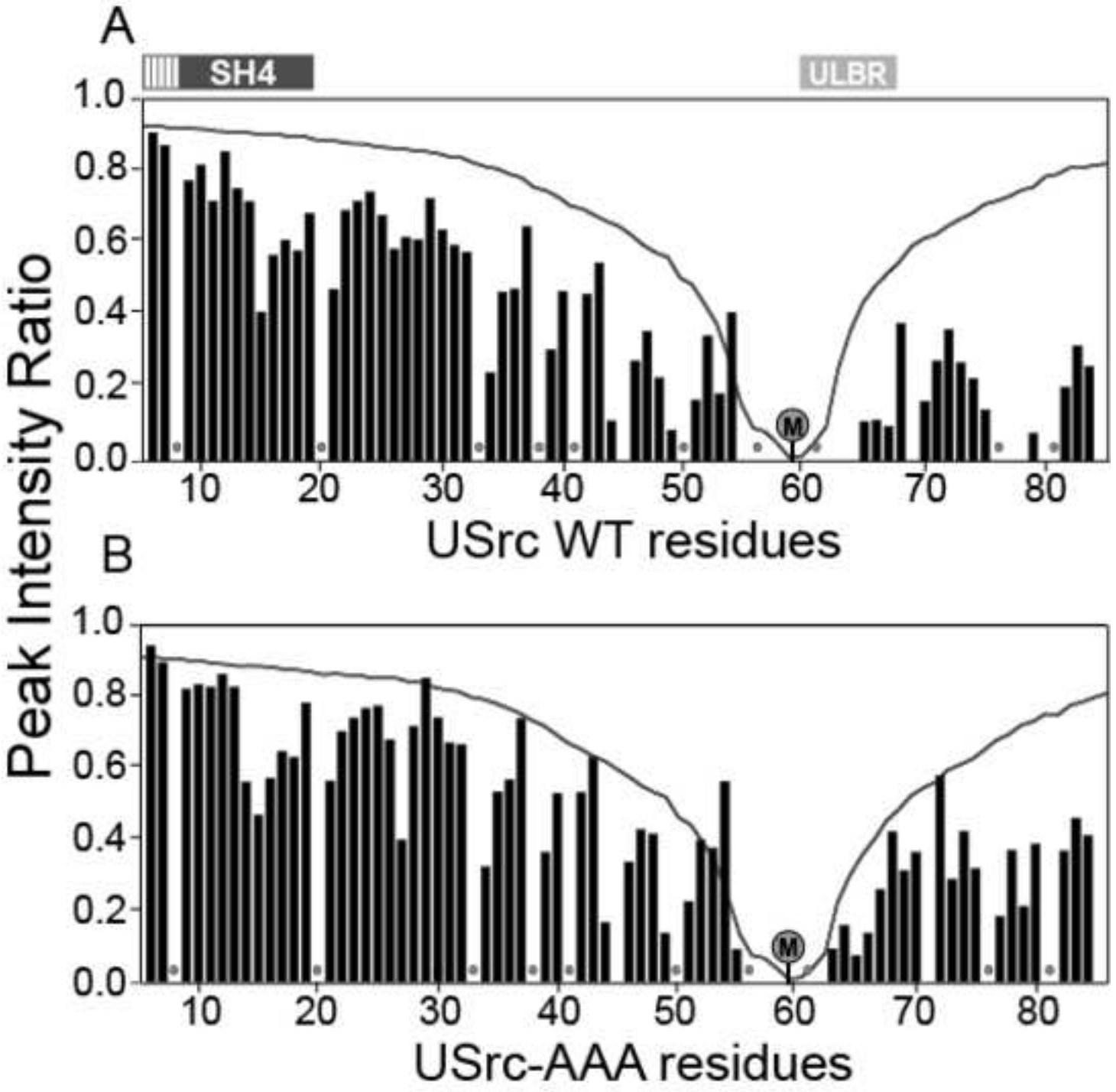

Figure
Click here to download high resolution image

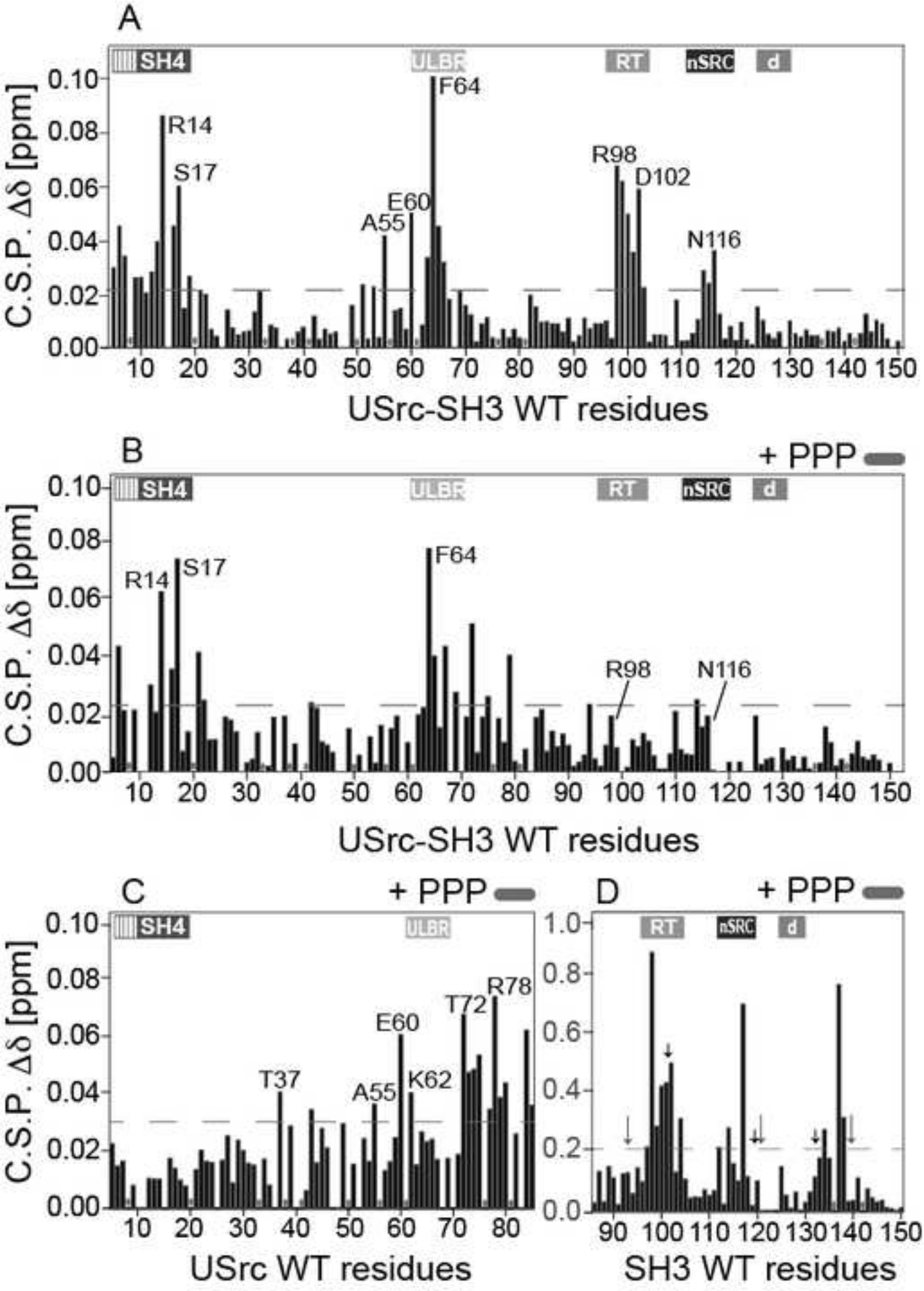

Figure
Click here to download high resolution image

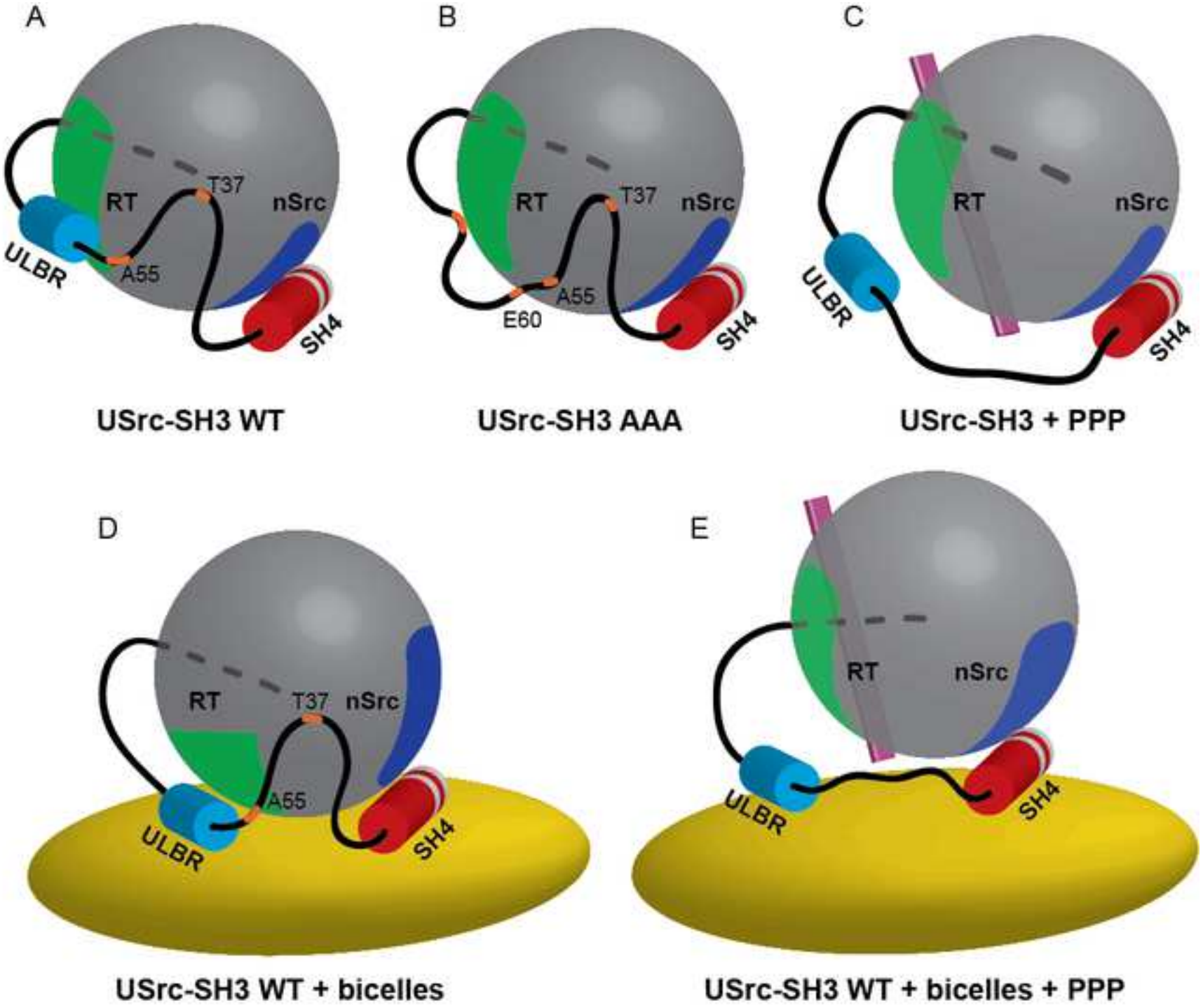

SUPPLEMENTAL FIGURES

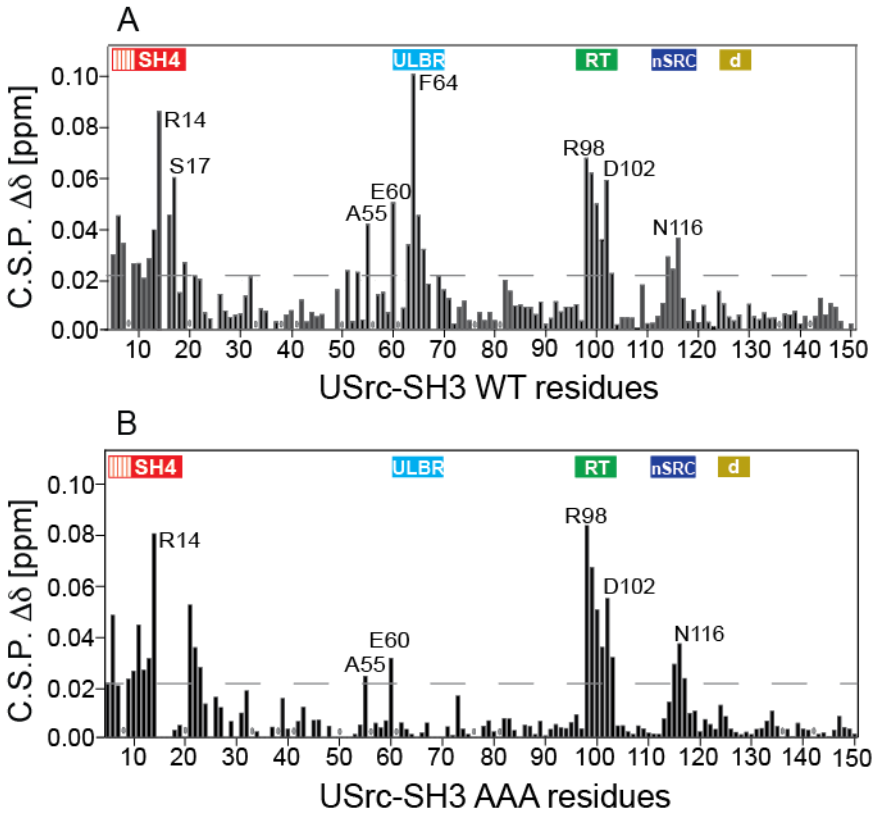

Figure S1. USrc-SH3-lipid interaction. (A,B) Combined ^{1}H-^{15}N chemical shift changes of USrc-SH3 WT (A) and USrc-SH3-AAA mutant (B) induced by the presence of 8% w/v of DHPC/DMPG bicelles. Grey circles indicate proline residues. The dashed line represents one standard deviation.

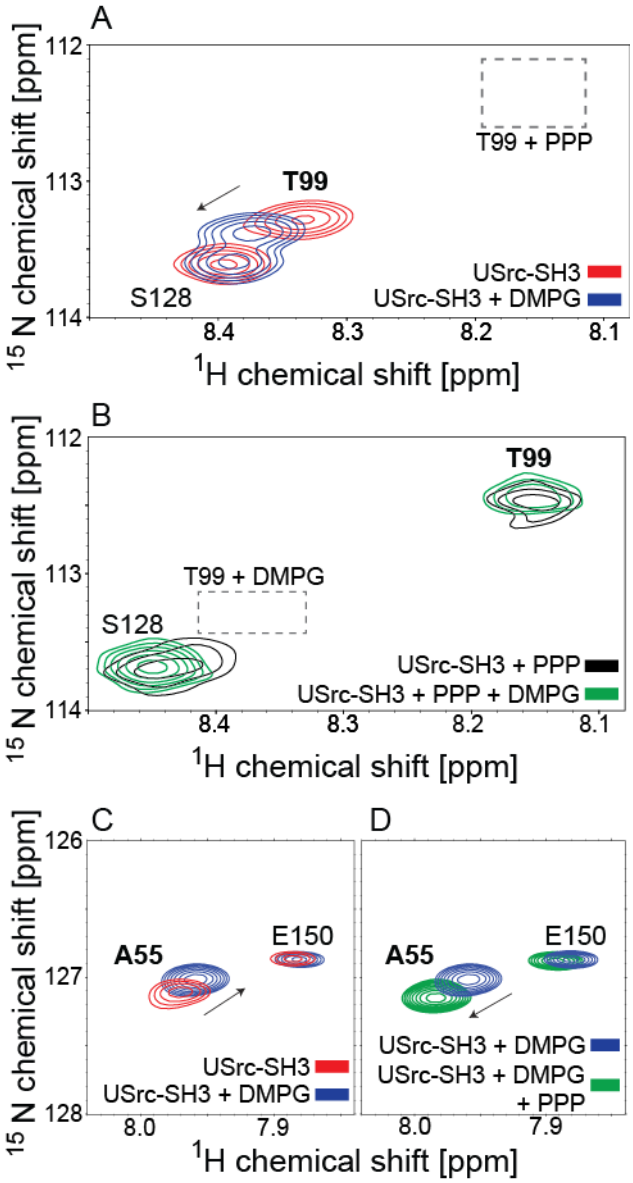

Figure S2. Effect of the Poly-Proline peptide on the SH3-lipid interaction. (A,B) Expansion of the T99 and S128 cross-peaks from ^{1}H-^{15}N HSQC NMR spectra of USrc-SH3 WT construct alone (red), in presence of negatively charged DHPC/DMPG bicelles (blue), in presence of PPP (black) and in presence of DHPC/DMPG and PPP (green). (C,D) Expansion of USrc-SH3 spectra showing residue A55 (UD) perturbed in the presence of DHPC/DMPG bicelles. This residue is successively affected by the addition of the VSL12 peptide resulting in the dissociation from the USrc-SH3-lipids complex to its unbound form.

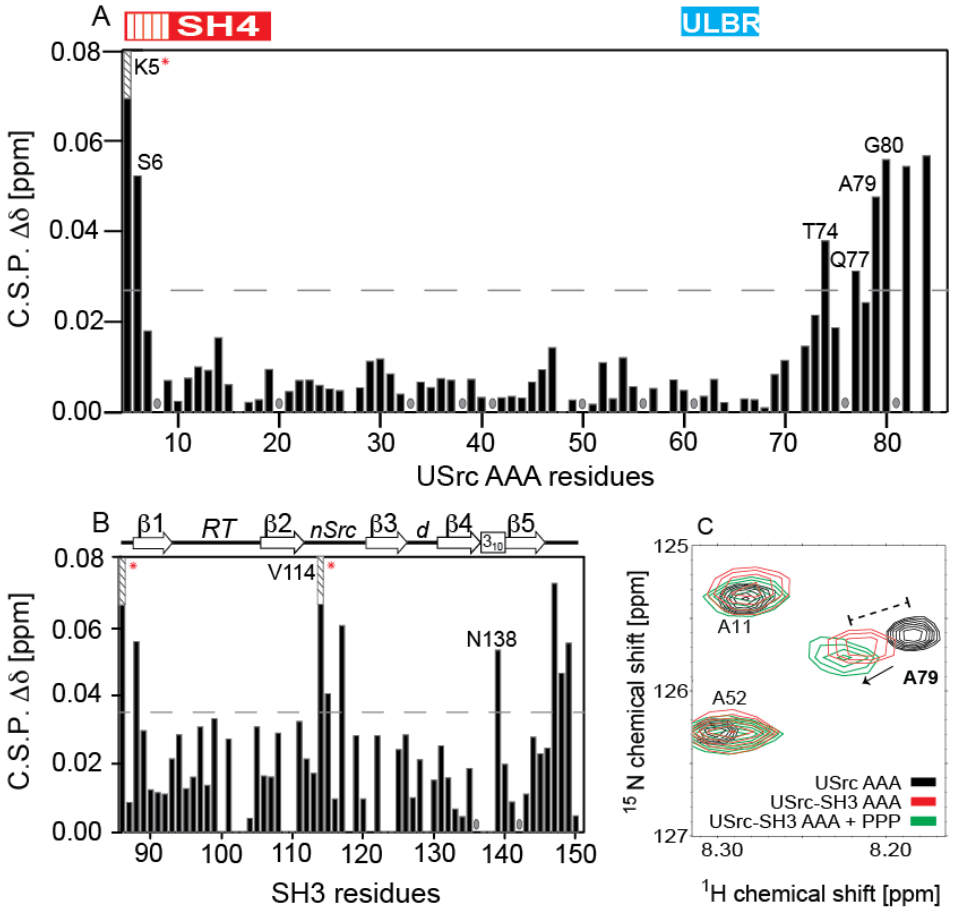

Figure S3. USrc-SH3-AAA inter-domain interaction in the presence of PPP. (A) Combined absolute value ^{1}H-^{15}N NMR chemical shift changes between linked and isolated domains in the presence of 1 equivalent of PPP. (A) USrc-SH3-AAA versus USrc-AAA at 278 K. (B) USrc-SH3-AAA versus SH3 at 298 K. K5* $\Delta\delta$ value is 0.14 ppm (A) and V86* $\Delta\delta$ value is 0.13 ppm (B). V114* $\Delta\delta$ value is 0.11 ppm. All spectra were measured at pH 7.0 and at a protein concentration of 0.2 mM. Combined NH chemical shift differences ($\Delta\delta$) were computed as in equation 1 (see Experimental Procedures). Gray circles indicate proline residues. The dashed line represents one standard deviation. (C) Expansion of A79 (Unique domain, hinge region) A52 (Unique domain) and A11 (SH4 domain) cross-peaks from ^{1}H-^{15}N HSQC NMR spectra of USrc-SH3-AAA construct alone (red), USrc-AAA alone (black) and USrc-SH3-AAA in presence of PPP (green).

SUPPLEMENTAL TABLE

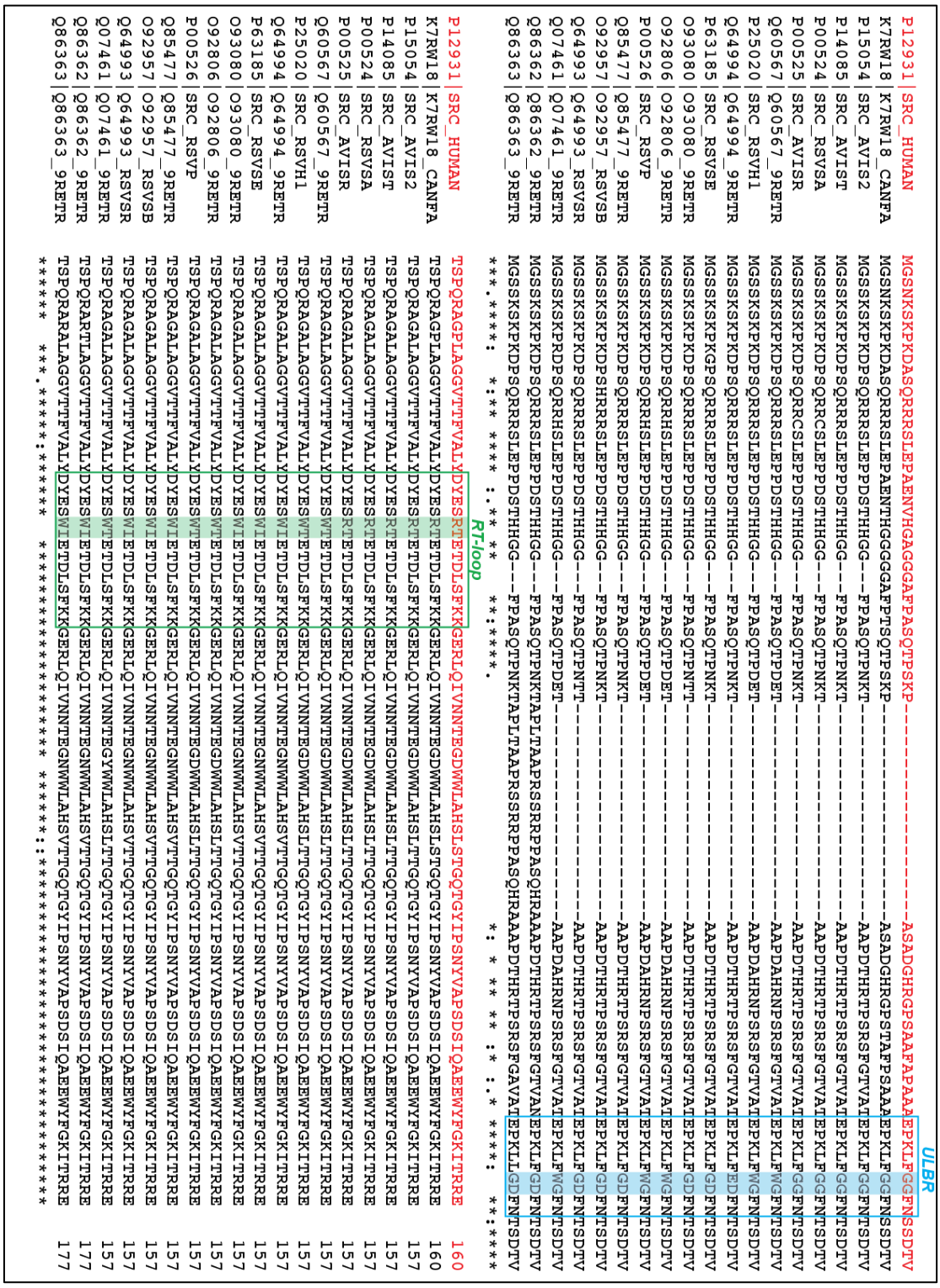

Table S1. v-Src sequence alignment. Multiple sequence alignment of the several strains of v-Src showing the first 177 residues. Human c-Src (Uniprot Entry P12931) USrc-SH3 sequence is shown in red as comparison. ULBR is highlighted in light blue. RT-loops are shown in green. UniProt entries correspond respectively to: K7RW18 - CANFA = V-src sarcoma Schmidt-Ruppin A-2 viral oncogene-like protein (DOG canis familiaris); P15054 - SRC_AVIS2 = Tyrosine-protein kinase transforming protein Src (Avian

sarcoma virus) (strain PR2257); P14085 - SRC_AVIST = Tyrosine-protein kinase transforming protein Src (Avian sarcoma virus) (strain S2); P00524 - SRC_RSVSA = Tyrosine-protein kinase transforming protein Src Avian leukosis virus RSA (RSV-SRA) (Rous sarcoma virus (strain Schmidt-Ruppin A); P00525 - SRC_AVISR = Tyrosine-protein kinase transforming protein Src (Avian sarcoma virus (strain rASV1441); Q60567 - 9RETR = V-3src-1 protein (Rous sarcoma virus); P25020 - SRC_RSVH1 = Tyrosine-protein kinase transforming protein Src (Rous sarcoma virus (strain H-19); Q64994 - 9RETR = (Schmidt-Ruppin D strain) v-src (Rous sarcoma virus); P63185 - SRC_RSVSE = Tyrosine-protein kinase transforming protein Src (Rous sarcoma virus (strain Schmidt-Ruppin E) (RSV-SR-E); O93080 - 9RETR = TsUP1 Src (Rous sarcoma virus); O92806 -9RETR = P60 src (Rous sarcoma virus); P00526 - SRC_RSVP = Tyrosine-protein kinase transforming protein Src (Rous sarcoma virus (strain Prague C) (RSV-PrC); Q85477 - 9RETR = Src (Rous sarcoma virus); O92957 - RSVSB = Src tyrosine kinase (Rous sarcoma virus (strain Schmidt-Ruppin B) (RSV-SRB); Q64993 - RSVSR = Tyrosine kinase (Rous sarcoma virus - Schmidt-Ruppin D); Q07461 - 9RETR = Src protein (Rous sarcoma virus); Q86362 - 9RETR = Pp62v (Rous sarcoma virus); Q86363 - 9RETR = Pp62v (Rous sarcoma virus). Sequence alignment was generated using Clustal Omega (EMBL-EBI).

Graphical Abstract

Click here to download high resolution image